Shorebird Patches as Fingerprints of Fractal Coastline Fluctuations due to Climate Change: Additional Files

M. Convertino,[1,2,3] A. Bockelie, [2,4,5] G.A. Kiker [1,3] R. Muñoz-Carpena, [1,3] I. Linkov [2,6]

[1] Department of Agricultural and Biological Engineering-IFAS, University of Florida, Gainesville, FL, USA

[2] Risk and Decision Science Team, Environmental Laboratory, Engineer Research and Development Center, US Army Corps of Engineers, Concord, MA, USA

[3] Florida Climate Institute, UF-FSU, c/o Frazier Rogers Hall, Gainesville, FL

[4] Department of Civil and Environmental Engineering, Massachusetts Institute of Technology, Cambridge, MA, USA

[5] Department of Earth, Atmospheric, and Planetary Science, Massachusetts Institute of Technology, Cambridge, MA, USA

[6] Department of Engineering and Public Policy, Carnegie Mellon University, Pittsburgh, PA, USA

August 17, 2012

Keywords: land cover change, coastal wetlands, coastline complexity, fractal dimension, habitat suitability, patches, sea-level rise

submitted to Ecological Processes - ***Special Issue on Wetlands In a Complex World, Guest Editor: Dr. Matteo Convertino***

Additional Methods

Maximum Likelihood Estimation of the Patch-size Probability

The Maximum Likelihood Estimation (MLE) method employed is fully described in Clauset et al. (2009). In this study, Pareto (power-law), truncated Pareto-Lévy (truncated power-law), and exponential distributions are tested for patch-size S which is the random variable of our interest. The appropriate MLE equation for the distribution of S is used to derive an exponent with the initial s_{min} parameter set to the minimum value found in the dataset. A best fit dataset is generated with the estimated parameters and a Kolmogorov-Smirnov (KS) test is used to determine the goodness of fit (the KS-D statistic). The KS test is the accepted test for measuring differences between continuous data sets (unbinned data distributions) that are a function of a single variable. This difference measure, the KS-D statistic, is defined as the maximum value of the absolute difference between two cumulative distribution functions. The D statistic between two different cumulative distribution functions $P_{N_1}(s)$ and $P_{N_2}(s)$ is defined by $D = \max_{-\infty<s<\infty} \mid P_{N_1}(s) - P_{N_2}(s) \mid$. To determine the best fit value for the s_{min} parameter the calculation is repeated with increasing values for s_{min} taken from the dataset with the value that resulted in the best (lowest) KS-D statistic being retained as the best fit value (Clauset et al., 2009; Humphries et al., 2010). When fitting a Pareto distribution the method is repeated to derive a best fit value for the s_{max} parameter, so for the Pareto distribution both the s_{min} and s_{max} parameters are fitted in the same way. We found that the Pareto-Lévy distribution (or commonly called "truncated power-law") is the best fit for the predicted distribution of the patch-size.

Additional Results and Discussion

The predicted land cover maps by the SLAMM model from 2006 to 2100 are represented in Figure S1. Many coastal wetland classes are considered into the land cover map. The Gulf of Mexico is divided into seven regions to which a unique set of SLAMM parameters is assigned (Table S1). A supporting video attached to this manuscript shows the predictions of the land cover in time. It appears that the East Apalachee Bay area (Zone 3 in the 2006 land cover map of Figure S1) and the South West area of the Gulf coast - North Everglades (Zone 7) will be largely inundated. The SLAMM class 17 represents the estuarine open water. The ocean open water is not represented in the maps. The zones 3 and 7 are subjected to the largest habitat transformations and loss. It is possible to see that the barrier islands in the South West area will be largely modified by the sea-level rise (SLR). The variation of the coastline

in those areas is large due to the low elevation and slope. The striped patterns observed in the East Apalachee Bay and in the South West areas are the result of the SLAMM model that considers exclusively the change of land cover from a cell with higher elevation to a cell with lower elevation, thus not affecting the neighboring cells (Chu-Agor et al., 2010). In Figure S2 the percentage of cells of each land cover class with respect to the total habitat is plotted in time. The global sea-level rise of 2 m produces local sea-level rise effects because of the different parameters assigned to each of the seven zones along the Florida coast and because of the natural heterogeneities of elevation and slope of each zone. Each land cover class - that represent also wetland types (swamp, cypress swamp, salt-marsh, and mangrove) - responds to sea-level rise differently according to the zonal geomorphological properties along the coast. A decrease in area in time is not observed for all the land cover classes. The smooth decline of the estuarine beach (10) and the mild increase of the ocean beach (12) reflect the quite smooth trend of the fractal dimension of the patches D_K for SNPL and REKN in time. As for the scrub/shrub (7) and salt marsh (8) classes, their rough and abrupt variations in time are observed also for the fractal dimension of the patches for the PIPL (Figure 5, b) which occupies also these habitats. It appears evident the direct association between geomorphological processes (simplified as land cover change) and biological processes (described as patches). A huge loss of the swamp (3) is observed, strong variations of the tidal flat (11), and a large increase of the estuarine open water due to the inundation and consequent loss of other habitat areas.

Figures S3, S4, and S5, show the suitability index (SI) for the breeding season of SNPL, and the wintering season of PIPL and REKN, in the Gulf coast of Florida from 2006 to 2100. The habitat suitability index is calculated as specified in the main text of the manuscript (see Methods). In Figures S3, S4, and S5 the patches are delineated according the proposed patch-delineation model and are reported below every Suitability Index map. A habitat patch is defined as a cluster of pixels that are good enough, big enough, and close enough together to support feeding and breeding by a particular species."Good enough" means that they have sufficient resources for the survivability of the species. "Big enough" reflects the fact that there is the need to have enough area to support at least one breeding unit, typically considered a mating pair of individuals with overlapping home ranges. "Close enough" means that the pixels must be clustered, rather than divided into a checkerboard by too much interspersion with pixels of bad habitat. By "a particular species" we emphasize the fact that one species' breeding patch may be another species' worst habitat patch. From the patterns of patches in Figures S3, S4, and S5, the variation of the patches is visible in time. The number of patches in the South-West Gulf coast of Florida is much higher for PIPL and

REKN than for SNPL, confirming the field data. The variation of the patches is larger for PIPL than for SNPL and REKN, especially in the Florida Peninsula coast.

The conditional probability in time of a SNPL breeding occurrence and of a PIPL and REKN adult occurrence in the winter season is shown in Figure S6 as a function of the predicted land cover (Figure S1) and the geology layers (Convertino et al., 2011b,a). The conditional probability changes as each environmental variable (land cover and geology) is varied, keeping all other environmental variables at their average sample value. In other words, the response curves of Figure S6 show the marginal effect of changing exactly one variable, whereas the model (MaxEnt) may take advantage of sets of variables changing together. The response curves are derived from the habitat suitability maps of Figures S3, S4, and S5. From the response curves it is possible to note the similarity of habitat preferences between the SNPL in the breeding season and the PIPL/REKN in the wintering seasons. SLAMM is the land cover according the SLAMM model classes and GEO is the geology layer (Convertino et al., 2011b,a). The Piping Plover seems to occupy also scrub/shrub transitional marsh and salt marsh areas (class 7, 8, and 9 respectively). The PIPL uses the ocean beach more than SNPL and REKN do (class 12). PIPL, and REKN, find more suitable substrates with medium/fine sand and silt (GEO class 4) and shelly sand and clay (GEO class 8). SNPL instead are found only in habitats characterized by white medium/fine sand and silt (class 4) that is typical of the Florida Gulf coast (Panhandle and Peninsula). It is not observed a significant variation in time of the conditional probabilities as a function of the environmental variables for the three TER species considered. The conditional probability to the geology layer shows more variation in time than for the land cover because the geology has been considered unchanged in time, thus the prediction is less reliable.

Figure S7 shows the number of patches vs. the average size of patches for SNPL, PIPL, and REKN. The dots are the binned average of all the realization for each year simulated. The plot shows how the number of patches N_p decreases with the size of patches $\langle s \rangle$ that increases. The PIPL has the smallest patches on average, while SNPL and REKN have similar patches of higher average size with respect to the PIPL.

References

Chu-Agor, M.L., R. Muñoz-Carpena, G.A. Kiker, A. Emanuelsson, and I. Linkov (2010) "Exploring sea-level rise vulnerability of coastal habitats using global sensitivity and uncertainty analysis," *Environmental Modeling and Software*, accepted.

Clauset, A., C.R. Shalizi, and M. E. J. Newman (2009) "Power-law distributions in empirical data," *SIAM Rev.*, Vol. 51, pp. 661 – 703.

Convertino, M., J.F. Donoghue, M.L. Chu-Agor, G.A. Kiker, R. Munoz-Carpena, R.A. Fischer, and I. Linkov (2011a) "Anthropogenic renourishment feedback on shorebirds: A multispecies Bayesian perspective," *Ecological Engineering*, Vol. 37, pp. 1184 – 1194.

Convertino, M., G.A. Kiker, R. Munoz-Carpena, M.L. Chu-Agor, R.A. Fischer, and I. Linkov (2011b) "Scale- and resolution-invariance of suitable geographic range for shorebird metapopulations," *Ecological Complexity*, Vol. 8, No. 4, pp. 364 – 376.

Humphries, N.E., N. Queiroz, J.R.M. Dyer, N.G. Pade, M.K. Musyl, K.M. Schaefer, D.W. Fuller, J.M. Brunnschweiler, T.K. Doyle, J.D.R. Houghton, G.C. Hays, C.S. Jones, L.R. Noble, V.J. Wearmouth, E.J. Southall, and D.W. Sims (2010) "Environmental context explains Lévy and Brownian movement patterns of marine predators," *Nature*, Vol. 465, No. 7301, pp. 1066–1069.

Additional Table Captions

Table S1. Land-cover model parameters. SLAMM model parameters for the 7 distinct geomorphological areas: Pensacola-Eglin (1), Tyndall (2), East Apalachee Bay (3), Big-Bend (4), Tampa Bay (5), Ft. Meyers (6), and North Everglades (7). The parameters that are different for each region are evidenced in grey.

Table S2. Model results. Fractal dimension of the patches D_K, number of patches N_p, mean patch size $\langle s \rangle$, mean number of connected patches $\langle c \rangle$ (that is a function of the estimated maximum dispersal distance d_l), for the TER-s species considered in the years 2006, 2020, 2040, 2060, 2080, and 2100.

Table S3. Comparison among fractal dimensions derived from different methods for the SNPL occurrences, and fractal dimension of the coastline. D_b, D_c, and D_K are the fractal dimension derived from the box-counting, the perimeter-area relationship, and the Korčak's law. The patch delineation model estimates (D_K) is validated in the period 2006-2010 against the observations (D_b). The relationship between D_f and D_b is the evidence of a correlation between geomorphological and ecological processes.

Additional Figure Captions

Figure S1. Simulated land cover patterns. Predicted land cover in time represented as SLAMM classes for the years 2006, 2020, 2040, 2060, 2080, and 2100. The domain has been divided into seven areas because different sea-level rise trend and tidal dynamics: Pensacola-Eglin (1), Tyndall (2), East Apalachee Bay (3), Big-Bend (4), Tampa Bay (5), Ft. Meyers (6), and North Everglades (7).

Figure S2. Predicted change of land cover in time. Variation in time of the land cover classes for the Gulf coast region modeled. (a) favorite habitat for SNPL, PIPL, REKN (estuarine beach (10) and ocean beach (12)). (b) land cover classes favorable for PIPL (scrub/shrub (7), salt marsh (8), and mangrove (9)). (c) other classes (undeveloped dryland (2), swamp (3), cypress swamp (4), inland fresh marsh (5), tidal flat (11), and estuarine open water (17)). Many classes of the land cover are coastal wetland types (salt-marsh, mangrove, swamp, and cypress swamp). The swamp is the type of costal wetlands that is experiencing the largest decay in area.

Figure S3. Simulated SNPL suitability index patterns. Suitability Index in time for the SNPL derived from the habitat suitability model (HSM) (MaxEnt) for the years 2006, 2020, 2040, 2060, 2080, and 2100. The suitable patches determined by the patch-delineation algorithm are represented.

Figure S4. Simulated PIPL suitability index patterns. Suitability Index in time and predicted patches for the PIPL derived from the HSM (MaxEnt) and the patch model for the years 2006, 2020, 2040, 2060, 2080, and 2100.

Figure S5. Simulated REKN suitability index patterns. Suitability Index in time and predicted patches for the REKN derived from the HSM (MaxEnt) and the patch model for the years 2006, 2020, 2040, 2060, 2080, and 2100.

Figure S6. MaxEnt response curves in time. Habitat suitability for breeding and wintering for SNPL, PIPL and REKN respectively, as a function of the land cover (as SLAMM classes) and geology classes calculated by MaxEnt for the years 2006, 2020, 2040, 2060, 2080, and 2100. The SLAMM classes are reported in Figure S2. The geology classes (GEO) are: clayey sand (1), gravel and coarse sand (2), limestone (3), medium/fine sand and silt (4), sandy clay and clay (5), shell beds (6), dolomite (7), shelly sand and clay (8), lime-

stone/dolomite (9), peat (10), and water (11).

Figure S7. Average number of patches vs. average size. N_p is the number of patches, and $\langle s \rangle$ is the average size. The dots are the binned average of the realizations for all the years modeled.

Additional Video

Video S1. Predicted land cover by SLAMM from 2006 to 2100.

Table S1:

	1	2	3	4	5	6	7
Direction of shore	S	S	S	W	W	W	W
Historic Trend (mm/yr)	2.1	0.75	1.38	1.8	2.36	2.4	2.02
Mean Tidal Level - NAVD88 (m)	0	0	0	0	0	0	0
Great Diurnal Tide Range (m)	0.383	0.409	0.492	1.158	0.688	0.401	0.874
Salt Elevation (m)	0.5745	0.6135	0.738	1.737	1.032	0.6015	1.311
Marsh Erosion (horz. m/yr)	2	2	2	2	2	2	2
Swamp Erosion (horz. m/yr)	1	1	1	1	1	1	1
Tidal Flat Erosion (horz. m/yr)	0.2	0.2	0.3	0.2	0.2	0.2	0.2
Regional Flood Marsh Accretion (mm/yr)	5.6	5.6	5.6	2.1	2.1	2.5	2.5
Irregular Flood Marsh Accretion (mm/yr)	3.75	3.75	3.76	3.75	3.75	3.75	3.75
Tidal Fresh Marsh Accretion (mm/yr)	4	4	4.2	4	4	4	4
Beach Sedimentation Rate (mm/yr)	0.3	0.3	0.3	0.3	0.3	0.3	0.3
Frequency Overwash (yr)	2	2	2	2	2	2	2
Max Width Overwash (m)	500	500	500	500	500	500	500
Beach to Ocean Overwash (m)	30	30	30	30	30	30	30
Dryland to Beach Overwash (m)	30	30	30	30	30	30	30
Estuary to Beach Overwash (m)	60	60	60	60	60	60	60
Marsh Pct. Loss Overwash (%)	50	50	50	50	50	50	50
Mangrove Pct. Loss Overwash (%)	25	25	25	25	25	25	25
Regional Flood Max Accretion. (mm/yr)	9	9	9	4.5	4.5	5.7	5.7
Reg. Flood Min Accretion (mm/yr)	4.7	4.7	4.7	1.4	1.4	1.4	1.4
Reg. Flood Diffusion Effect Max (m)	0	0	0	0	0	0	0
Reg. Flood Diffusion Effect Min (-)	1	1	1	1	1	1	1
Reg. Flood Salinity Turbulence Max (ppt)	0	0	0	0	0	0	0
Reg. Flood Turbulence Max Zone (ppt)	0	0	0	0	0	0	0
Reg. Flood Salinity Non Turb. Max (-)	1	1	1	1	1	1	1

Table S2:

	2006	2020	2040	2060	2080	2100
			Snowy Plover			
D_K	1.47	1.576	1.582	1.54	1.573	1.55
N_p	219	182	206	226	304	312
$\langle s \rangle$	10.37	9.38	8.48	8.32	7.59	7.92
$\langle c \rangle$	5	7	7	6	9	8
			Piping Plover			
D_K	1.7	1.64	1.646	1.356	1.595	1.733
N_p	369	550	357	403	996	692
$\langle s \rangle$ (km^2)	6.48	7.03	6.33	6.31	11.12	5.81
$\langle c \rangle$ (km)	12	10	11	9	10	20
			Red Knot			
D_K	1.42	1.452	1.464	1.469	1.617	1.56
N_p	189	220	177	199	272	320
$\langle s \rangle$ (km^2)	11.30	10	9.89	9.52	7.59	7.90
$\langle c \rangle$ (km)	11	13	13	15	18	18

Table S3:

	2002	2003	2004	2005	2006	2007	2008	2009	2010
D_f	1.26	1.28	1.37	1.35	1.29	1.29	1.30	1.32	1.33
	Snowy Plover								
D_b	1.63	1.62	1.75	1.74	1.63	1.64	1.66	1.68	1.70
D_c	–	–	–	–	1.52	1.53	1.58	1.61	1.65
D_K	–	–	–	–	1.47	1.49	1.52	1.54	1.58

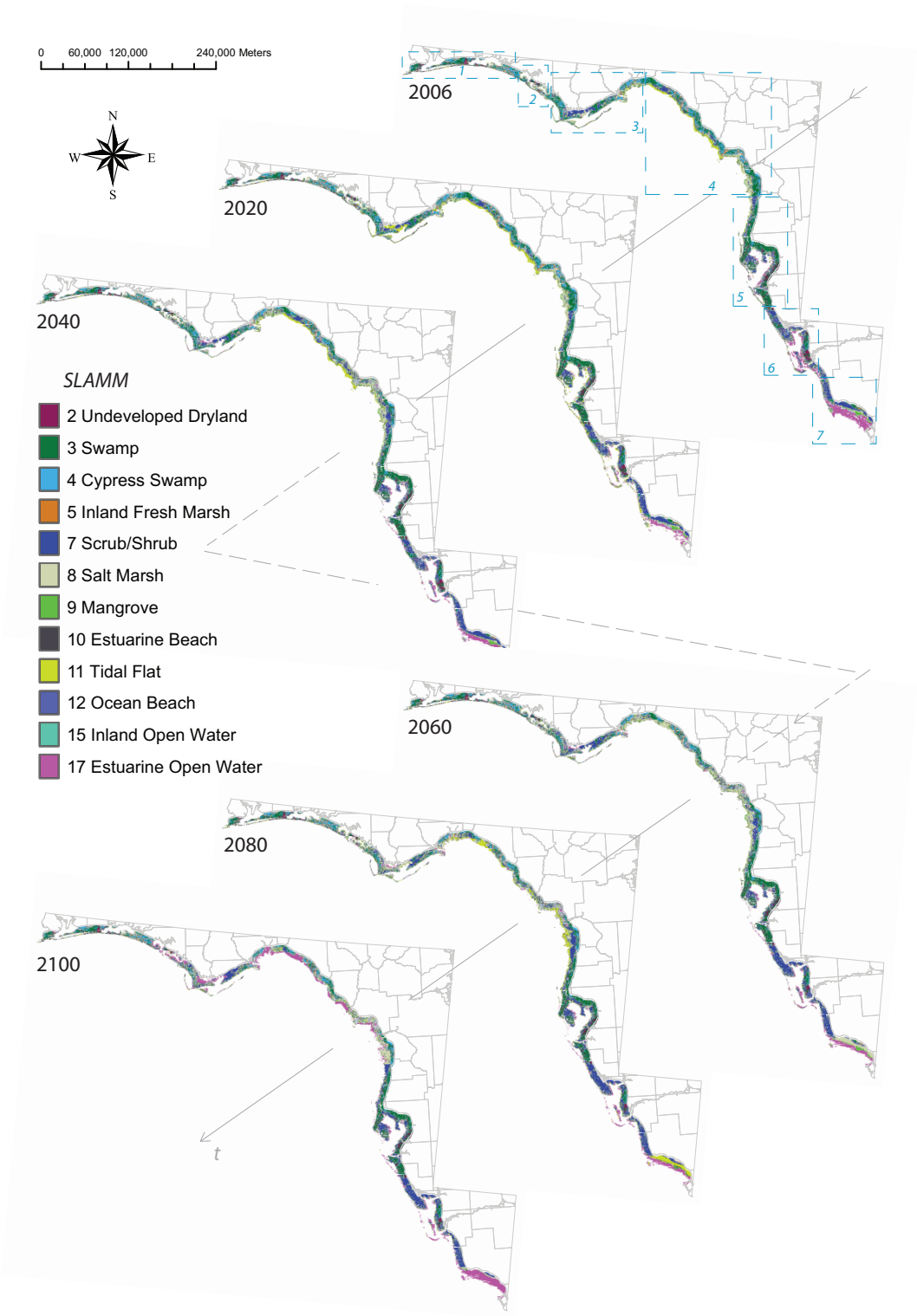
0 60,000 120,000 240,000 Meters
N
W
E
S
2006
2020
2040
2060
2080
2100
SLAMM
2 Undeveloped Dryland
3 Swamp
4 Cypress Swamp
5 Inland Fresh Marsh
7 Scrub/Shrub
8 Salt Marsh
9 Mangrove
10 Estuarine Beach
11 Tidal Flat
12 Ocean Beach
15 Inland Open Water
17 Estuarine Open Water
t

Figure S1:

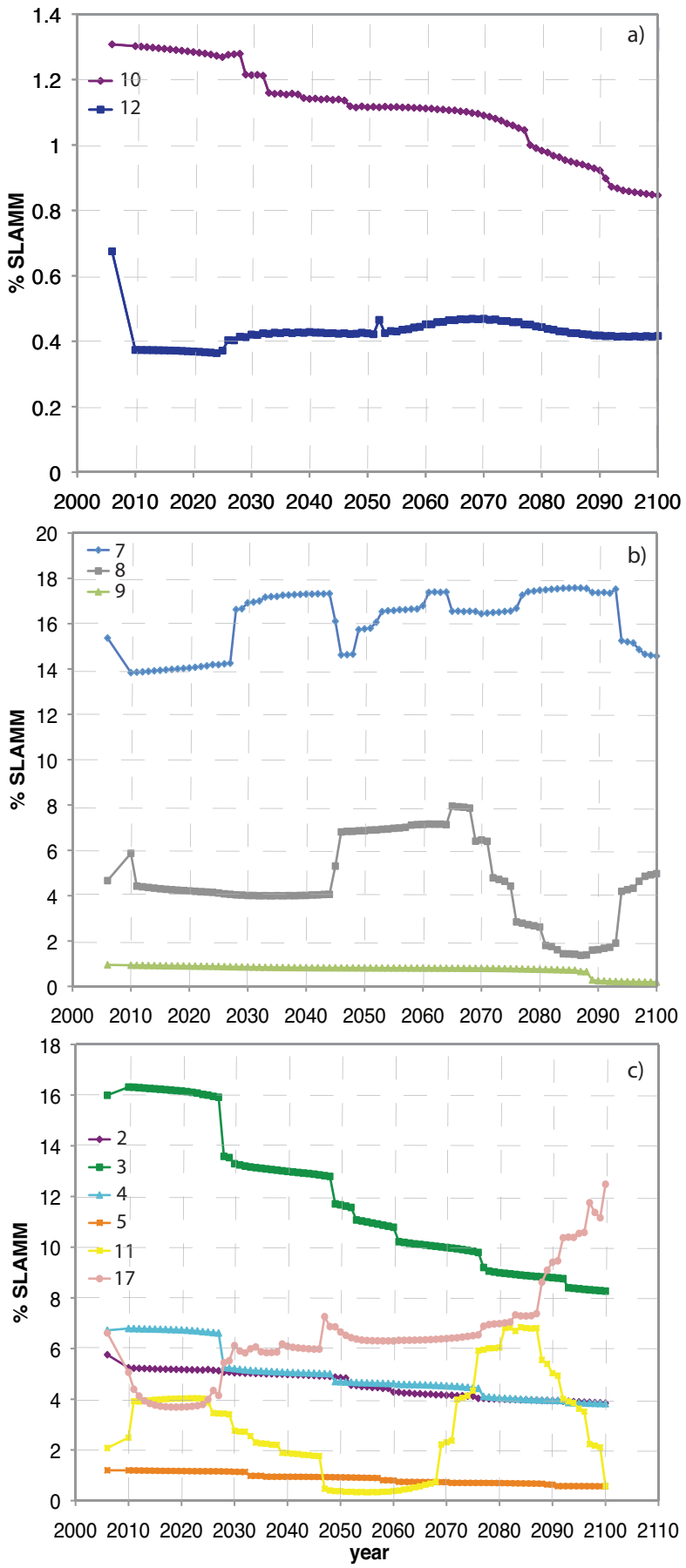

Figure S2:

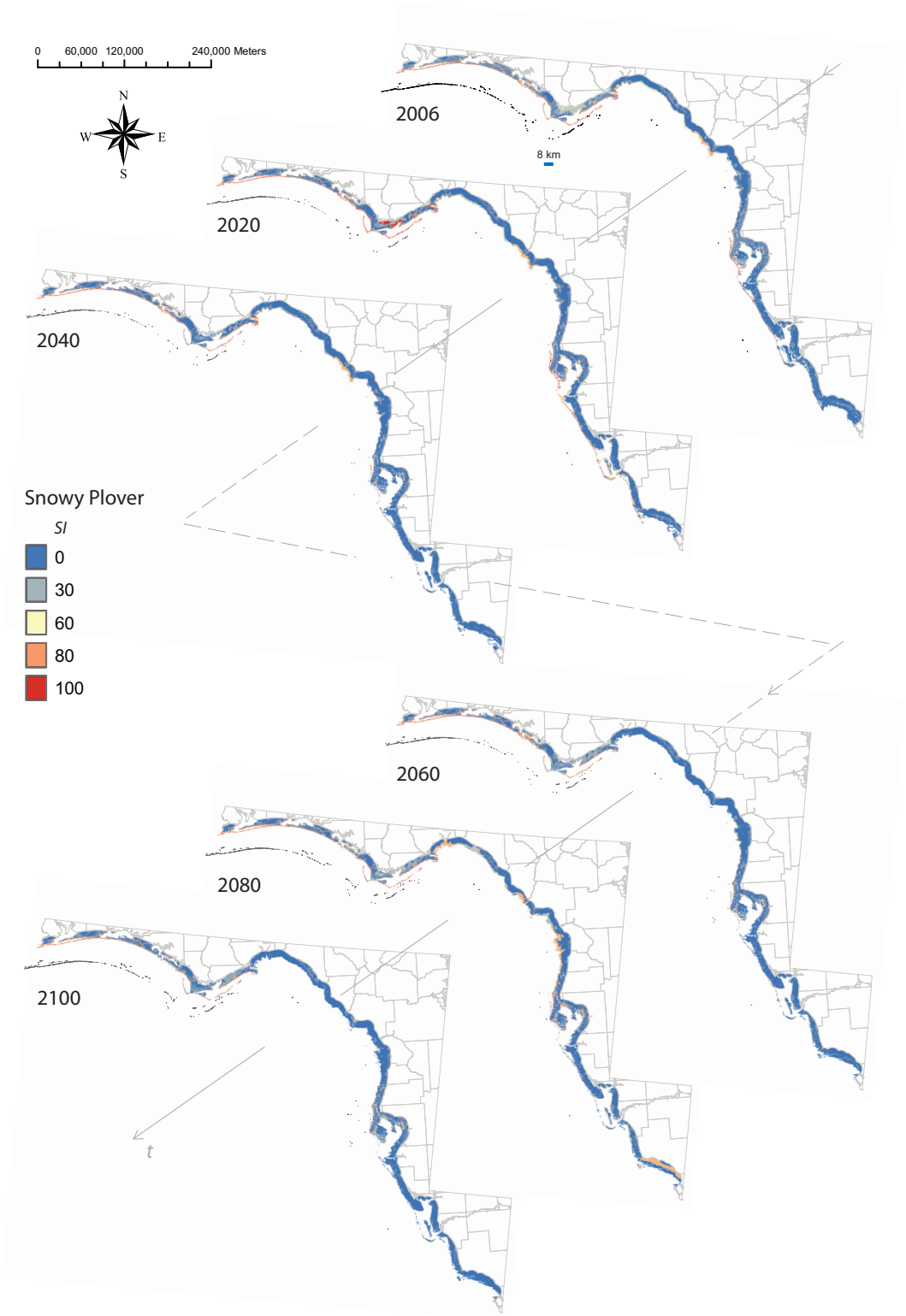
0
60,000
120,000
240,000 Meters
N
W
E
S
8 km
2006
2020
2040
2060
2080
2100
t
Snowy Plover
SI
0
30
60
80
100

Figure S3:

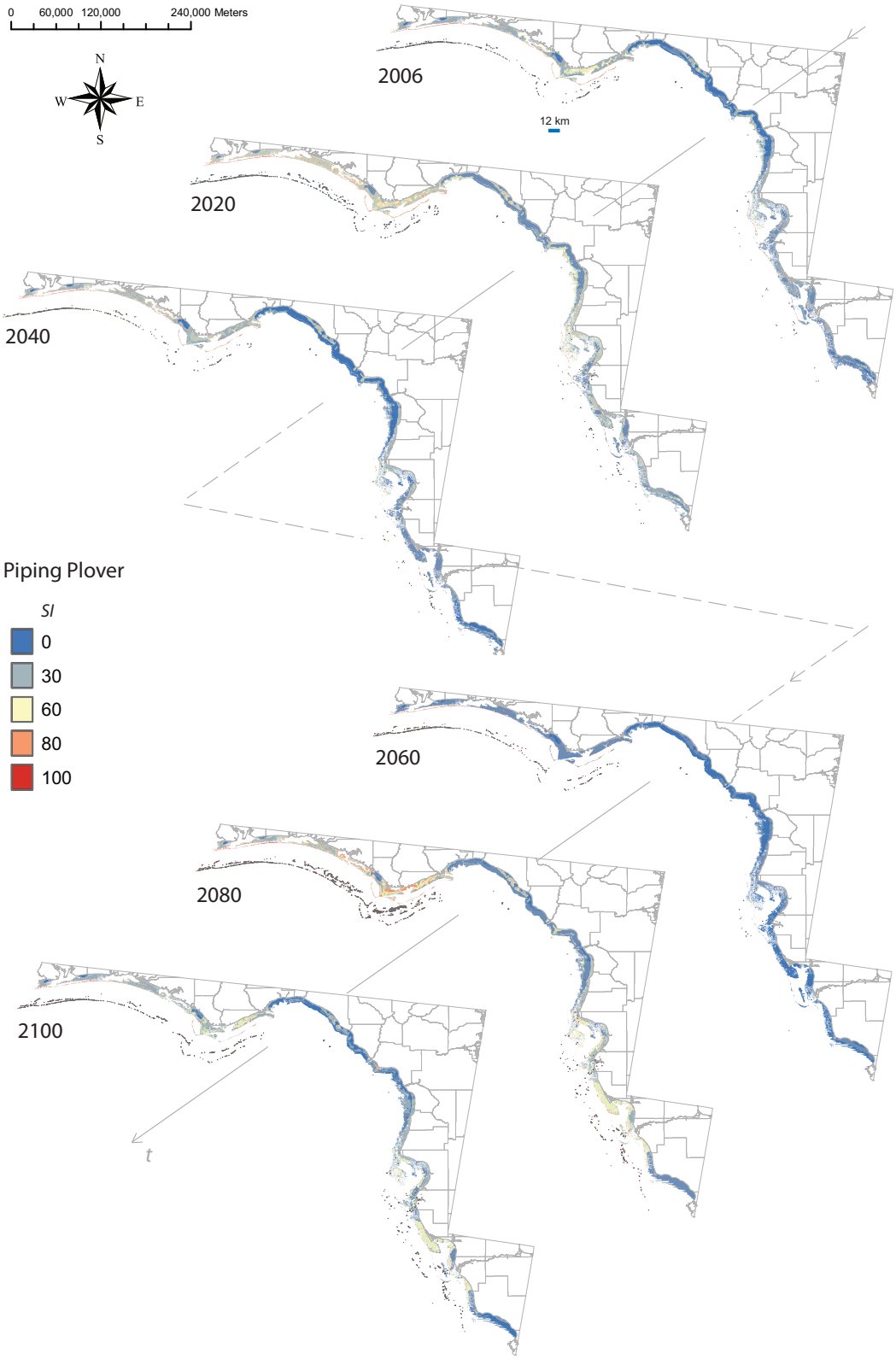
0 60,000 120,000 240,000 Meters
N
W
E
S
12 km
2006
2020
2040
2060
2080
2100
t
Piping Plover
SI
0
30
60
80
100

Figure S4:

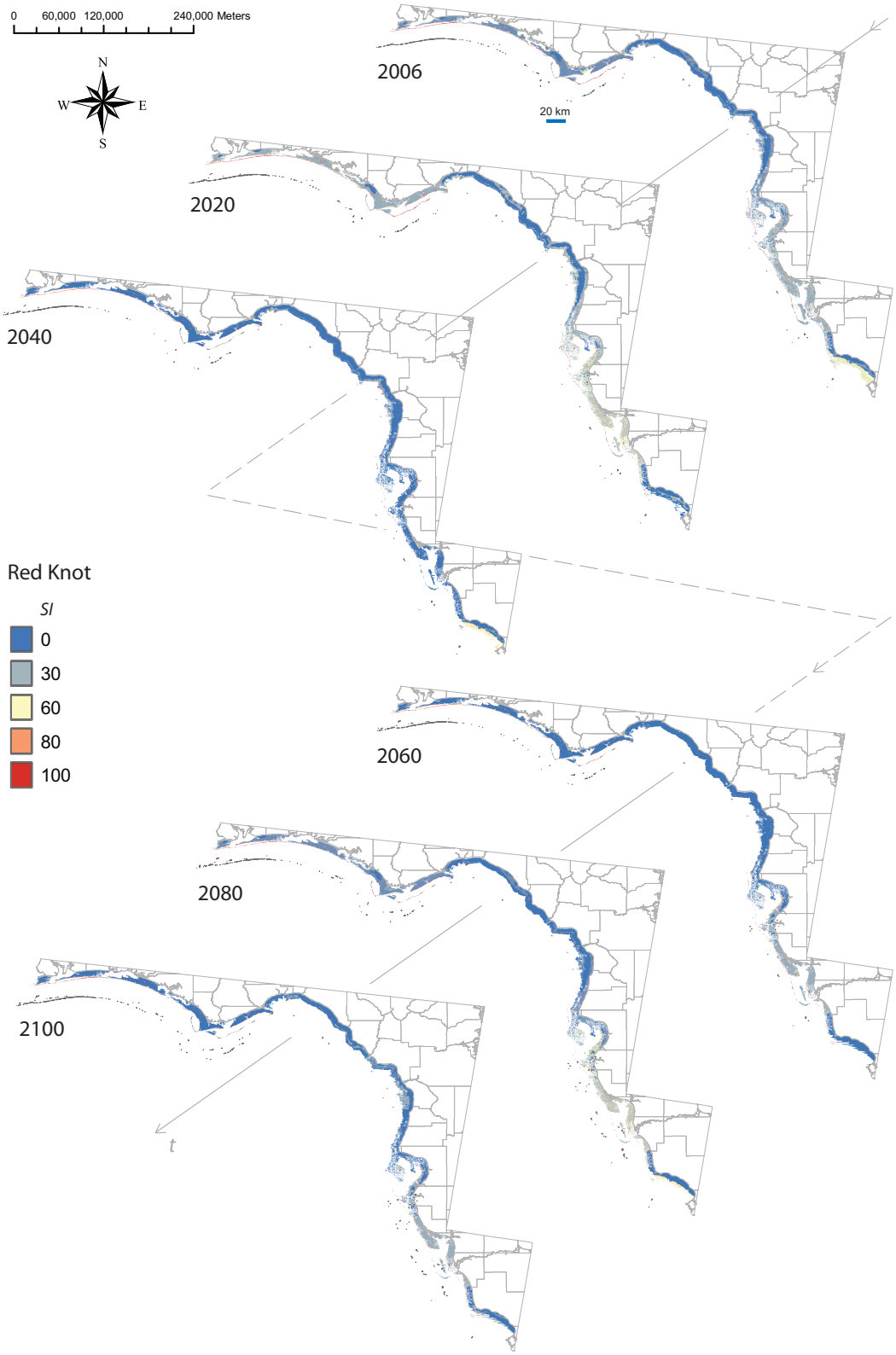
0
60,000
120,000
240,000 Meters
N
W
E
S
2006
20 km
2020
2040
Red Knot
SI
0
30
60
80
100
2060
2080
2100
t

Figure S5:

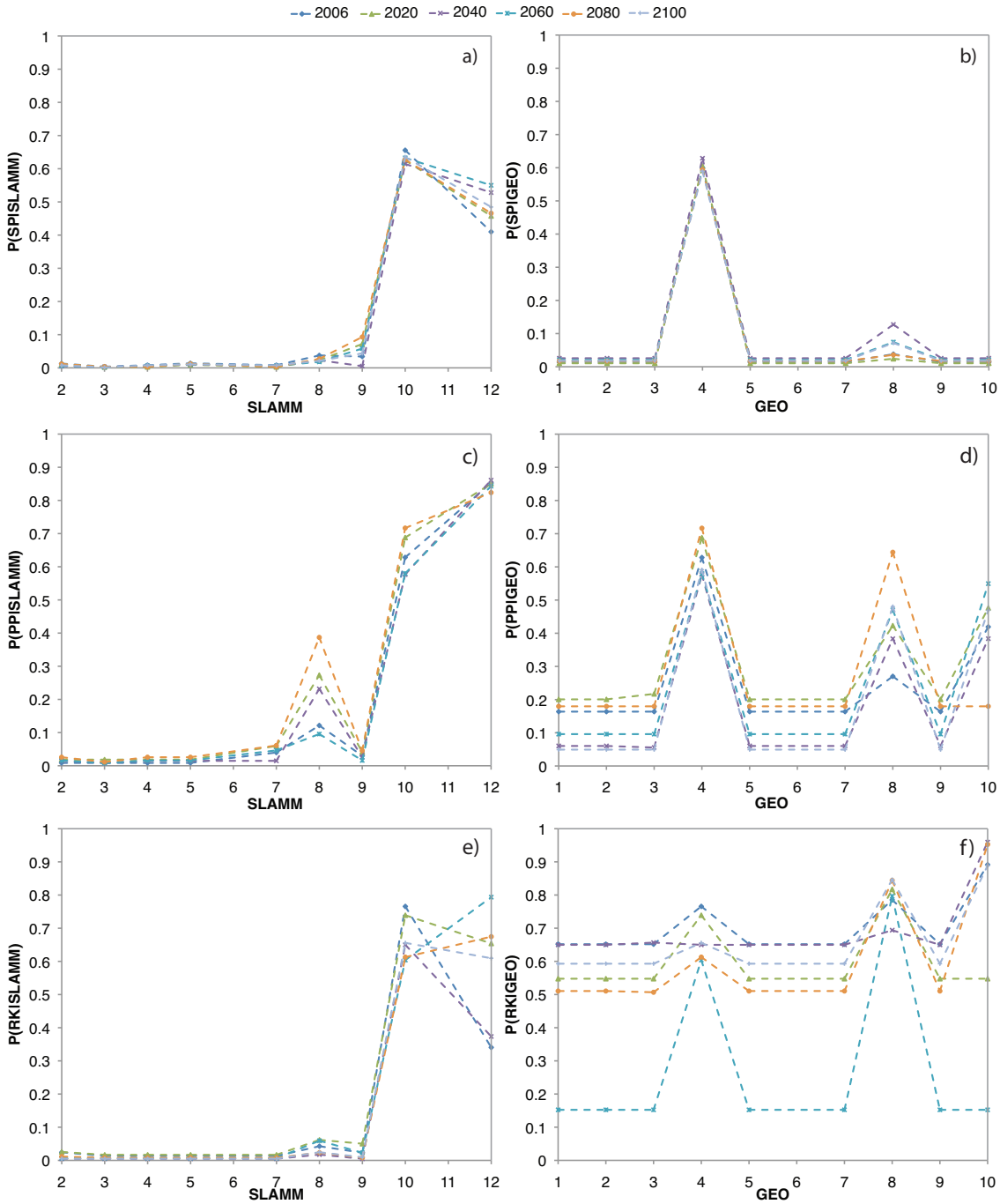
2006
2020
2040
2060
2080
2100
a)
b)
c)
d)
e)
f)
P(SPISLAMM)
P(SPIGEO)
P(PPISLAMM)
P(PPIGEO)
P(RKISLAMM)
P(RKIGEO)
SLAMM
GEO

Figure S6:

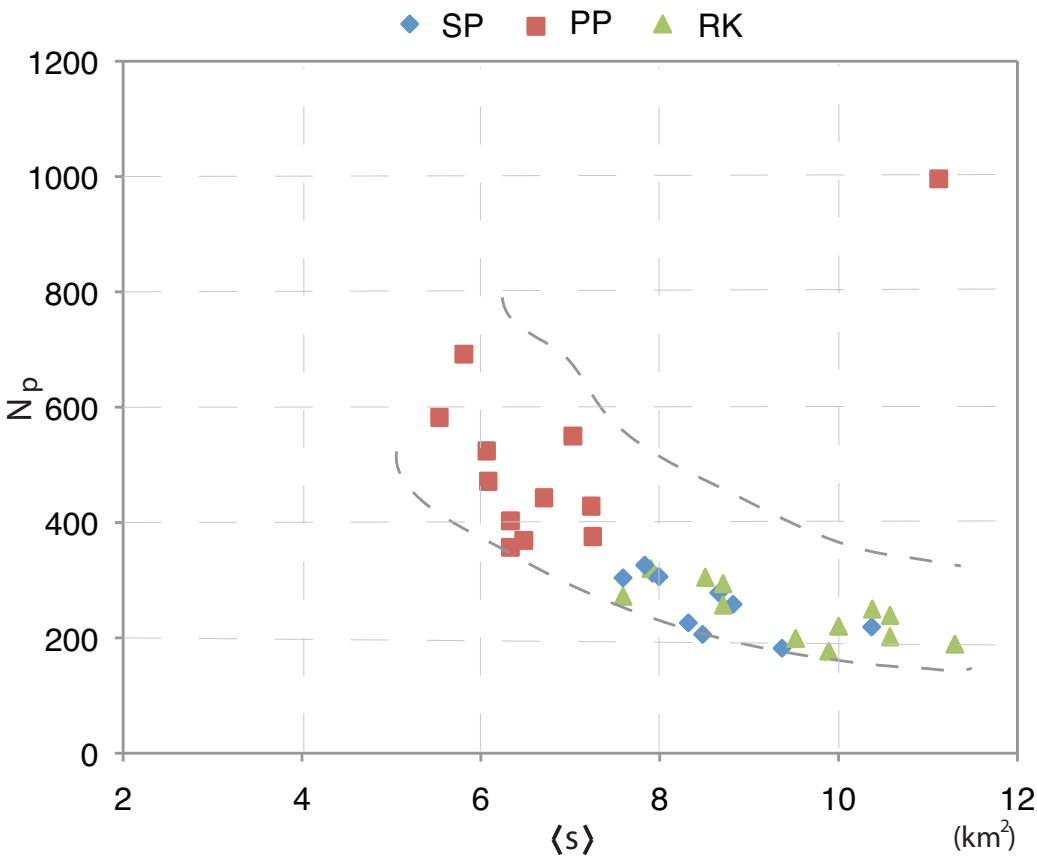

Figure S7: